Optimal Routing for Quantum Networks

Article in IEEE Access · October 2017

DOI: 10.1109/ACCESS.2017.2763325

1 author:

Marcello Caleffi
University of Naples Federico II

IEEE Access
Multidisciplinary : Rapid Review : Open Access Journal

Received September 27, 2017, accepted October 11, 2017, date of publication October 16, 2017, date of current version November 7, 2017.

Digital Object Identifier 10.1109/ACCESS.2017.2763325

Optimal Routing for Quantum Networks

MARCELLO CALEFFI, (Senior Member, IEEE)
National Laboratory of Multimedia Communications, National Inter-University Consortium for Telecommunications, 80126 Naples, Italy
Department of Electrical Engineering and Information Technologies, University of Naples Federico II, 80125 Naples, Italy
e-mail: marcello.caleffi@unina.it

ABSTRACT To fully unleash the potentials of quantum computing, several new challenges and open problems need to be addressed. From a routing perspective, the *optimal routing problem*, i.e., the problem of jointly designing a routing protocol and a route metric assuring the discovery of the route providing the highest quantum communication opportunities between an arbitrary couple of quantum devices, is crucial. In this paper, the *optimal routing problem* is addressed for generic quantum network architectures composed by repeaters operating through single atoms in optical cavities. Specifically, we first model the entanglement generation through a stochastic framework that allows us to jointly account for the key physical-mechanisms affecting the end-to-end entanglement rate, such as decoherence time, atom–photon and photon–photon entanglement generation, entanglement swapping, and imperfect Bell-state measurement. Then, we derive the closed-form expression of the *end-to-end entanglement rate* for an arbitrary path and we design an efficient algorithm for entanglement rate computation. Finally, we design a routing protocol and we prove its optimality when used in conjunction with the entanglement rate as routing metric.

INDEX TERMS Quantum networks, quantum routing, entanglement rate, route metric, optimal routing.

I. INTRODUCTION

Very recently, researchers worldwide have started to devote massive efforts in designing and implementing quantum computation [1], with 17-qubit computing processors already prototyped [2] and several groups making very fast progress towards the 50-qubit regime [3], [4].

To fully unleash the ultimate vision of the quantum revolution, it is necessary to design and to implement *quantum networks* [5], [6], able to connect distant quantum processors through remote quantum entanglement[1] distribution. However, despite the tremendous progress of quantum technologies, long-distance efficient entanglement distribution still constitutes a key issue, due to the exponential decay of communication rate as a function of the distance [7], [8].

A solution for counteracting the exponential decay loss is the adoption of *quantum repeaters* [9], [10]. As shown in Figure 1, instead of distributing entanglement over a long link, entanglement will be generated through smaller links. A combination of *entanglement swapping* [11] and *entanglement purification* [12] performed at each quantum repeater enables the extension of the entanglement over the entire channel.

By looking at Figure 1, a simple question arises spontaneously: *"when does a repeater assure higher entanglement distribution over the direct long link?"*. Or equivalently, by adopting a networking terminology, *"given that there are two available paths, a direct path between nodes v_1 and v_3 and an indirect path through repeater v_2, which is the path assuring the higher entanglement distribution?"*

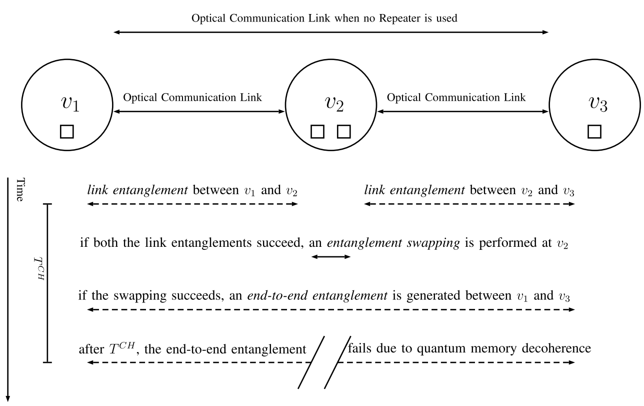

FIGURE 1. Schematic illustration of the end-to-end entanglement generation between nodes v_1 and v_3 through quantum repeater v_2, with quantum memories depicted as squares and T^{CH} denoting the decoherence time. Time duration proportion among operations not respected for the sake of clarity.

Indeed, as we will show through the manuscript, answering this question is very challenging, due to the complex and stochastic nature of the physical mechanisms underlying quantum entanglement. Furthermore, quantum entanglement is affected by an additional key-issue: *quantum decoherence*,

[1]For a short introduction of quantum entanglement and the related concepts please refer to Section II-A.

which involves a loss of the entanglement between the entangled entities as time passes.

Hence, in this paper, we address the aforementioned optimal routing problem by jointly designing a routing protocol and a route metric able to account for the distinguishable properties of quantum networks.

More specifically, we first develop an analytical framework to model the entanglement generation process, by explicitly taking into account the key physical-mechanisms affecting the entanglement generation in cavity-based quantum networks, such as decoherence time, atom-photon and photon-photon entanglement generation, entanglement swapping, and imperfect Bell-state measurement. Then, we analytically derive the closed-form expression of the entanglement rate through an arbitrary path. Finally, we design a link-state routing protocol based on path enumeration, and we prove its optimality when used in conjunction with a routing metric based on the entanglement rate by means of the routing algebra theory.

The rest of the paper is organized as follows. In Section II, we present the problem statement and we highlight the contributions of this paper. In Section III, we describe the network model along with some preliminaries. In Section IV, we analytically derive the closed-form expression of the *end-to-end entanglement rate* and we design the optimal routing protocol. In Section V, we evaluate the rate under realistic parameter setting and we analyze the performance degradation induced by the lack of routing optimality. In Section VI, we conclude the paper, whereas some proofs are gathered in the Appendix.

II. PROBLEM STATEMENT

A. PRELIMINARIES

Differently from classical information, quantum information (e.g., qubits) cannot be copied due to the *no-cloning theorem* [13], [14]. Hence, quantum networks rely on the *quantum teleportation* process [15] as the unique feasible solution to *transmit* a qubit without the need of physically moving the physical particle storing such a qubit.

The quantum teleportation of a single qubit between two different nodes requires: i) a classical communication channel capable of sending two classical bits, and ii) the generation of a pair of maximally entangled[2] qubits, referred to as *EPR pair*, with each qubit stored at each remote node. In the following, the generation of an EPR pair at two different nodes is referred to as *remote entanglement generation*.

In a nutshell, the process of teleporting an arbitrary qubit, say[3] qubit $|\varphi\rangle$, from quantum node v_i to quantum node v_j can be summarized as follows:

i) an EPR pair, i.e., a remote entanglement, is generated between v_i and v_j, with first qubit $|\Phi_i\rangle$ stored at v_i and second qubit $|\Phi_j\rangle$ stored at v_j;
ii) at v_i, a Bell-state measurement[4] of $|\Phi_i\rangle$ and $|\varphi\rangle$ is performed, and the 2-bits measurement output is sent to v_j through the classical communication channel;
iv) by manipulating the EPR pair qubit $|\Phi_j\rangle$ at v_j on the basis of the received measurement output, the qubit $|\varphi\rangle$ is obtained.

B. CHALLENGES

From the description above, it becomes clear that the design of a routing metric for quantum networks poses several challenges:

- *Entanglement*. As in classical networks, the transmission of quantum information is limited by the classical bit throughput, necessary to transmit the output of the Bell-state measurement. But, differently from classical networks, the transmission of quantum information requires the generation of a remote entanglement. Hence, a quantum routing metric must jointly account for both these two limiting factors.
- *Decoherence*. Not only entanglement is the most valuable resource for transmitting quantum information, but it is also a perishable resource. Indeed, due to the inevitable interactions with the external environment, there exists a loss of the entanglement between the entangled entities as time passes. Hence, a quantum routing metric must explicitly account for the quantum decoherence.
- *Stochasticity*. The physical mechanisms underlying the entanglement generation are stochastic. Hence, a quantum routing metric must be able to effectively describe such a stochastic nature.

Remark 1: Indeed, due to the difficulties arising from entanglement generation and quantum decoherence, entanglement can be considered the *key limiting factor* for quantum information transmission. In fact, the qubit transmission rate between two quantum nodes is upper bounded by the entanglement generation rate, since each qubit teleportation requires a successfully remote entanglement generation. Hence, through the paper, we design a routing metric for quantum networks based on the entanglement rate.

C. ROUTE METRIC DESIGN

By taking into account the aforementioned challenges, in this paper, we design a route metric for quantum networks exhibiting the following attractive features:

1) The metric is *entanglement-aware*, i.e., it accounts for the need of remote entanglement generation in quantum information transmission;
2) The metric is *accurate*, i.e., it accounts for all the physical-mechanisms affecting the entanglement

[2] Two qubits are entangled when their state can not be described as the tensor product of the state of qubits. An EPR pair is a pair of qubits that are maximally entangled with each other, i.e., that are in one of the four Bell states together. Generally, the four Bell states are denoted with $\Phi^+, \Phi^-, \Psi^+, \Psi^-$.

[3] The *ket* notation $|\cdot\rangle$ is a standard notation for representing qubits states.

[4] A Bell-state measurement is a joint quantum measurement of two qubits for determining which of the four Bell states the two qubits are in.

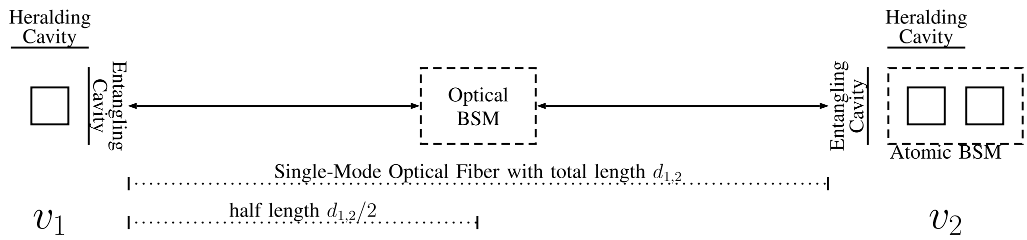

FIGURE 2. Schematic illustration of the adopted quantum network architecture, operating through single atoms in optical cavities. Dimension proportion among different components not respected for the sake of clarity.

generation, such as decoherence time, atom-photon and photon-photon entanglement generation, entanglement swapping and imperfect Bell-state measurement.

3) The metric is *stochastic*, i.e., it is able to effectively describe the stochastic nature of the physical mechanisms underlying the entanglement generation.

More in detail, we first develop a stochastic framework to model the entanglement generation. As opposed to existing literature [16]–[20], we jointly account for all the key physical-mechanisms affecting the end-to-end entanglement rate, such as decoherence time, atom-photon and photon-photon entanglement generation, entanglement swapping and imperfect Bell-state measurement. Then, we analytically derive the closed-form expression of the entanglement rate, first through a link and then through an arbitrary path. We also design an efficient algorithm for entanglement rate computation, exhibiting a linearithmic time complexity.

Finally, we design a link-state-based routing protocol and we prove its optimality when used in conjunction with the entanglement rate as routing metric by means of the routing algebra theory.

III. MODEL AND PRELIMINARIES

Here, we first introduce the quantum network architecture in Section III-A. Then, in Section III-B, we describe the network model and we collect several definitions that will be used throughout the paper.

A. NETWORK ARCHITECTURE

We consider without loss of generality[5] a wired quantum network composed by repeaters operating through single atoms in optical cavities. The entanglement generation is based on single-photon detection and high-fidelity entangled pairs are created at the price of low entanglement generation success probabilities [20], [22]–[25].

Specifically, as shown in Figure 2, a quantum repeater consists of an atom storing a qubit and surrounded by two cavities: an *heralding cavity* and a *telecom-wavelength entangling cavity*. The atoms (^{87}Rb rubidium isotopes) are individually excited by laser pulses, which allows the entanglement between the atom and a telecom-wavelength photon.[6] More in detail, the heralding cavity is responsible for detecting the entanglement generation, whereas the entangling cavity is responsible for coupling the telecom-wavelength photon to the mode of a single-mode optical telecom fiber.

Once an atom-photon entanglement is locally generated at each node, a remote entanglement between two adjacent nodes[7] is generated by entanglement swapping through *optical Bell-State Measurement (BSM)* of the two photons.

Finally, remote entanglement between non-adjacent nodes is generated by performing entanglement swapping at intermediate nodes through an *atomic BSM* operating on the atom pair stored at each intermediate node. Specifically, cavity-assisted quantum gate is performed on the two atoms via reflection of a single photon originating from a cavity-based single-photon source (SPS). Subsequent detection of the atomic quantum states in suitable bases allows for an unambiguous determination of the two-particles Bell state. This results in an entangled state between the two non-adjacent nodes.

B. NETWORK MODEL

We denote the quantum network with the graph $G = (V, E)$, with $V = \{v_i\}_{i=1}^{N}$ and $E = \{e_{i,j},\ v_i, v_j \in V\}$ denoting the set of nodes and optical links, respectively.

Given an arbitrary couple of nodes v_i and v_j, if it exists $e_{i,j} \in E$ then v_i and v_j are defined *adjacent* nodes. Furthermore, $d_{i,j}$ and $T^{\mathrm{c}}_{i,j}$ denote the length of the optical link and the average time[8] required for a classical communication between node v_i and v_j, respectively.

The route $r_{i,j}$ denotes a simple path between two arbitrary nodes v_i and v_j, i.e., a finite ordered sequence of edges $(e_{\sigma_1,\sigma_2}, \ldots, e_{\sigma_{n-1},\sigma_n})$ in E so that $v_{\sigma_1} = v_i$, $v_{\sigma_n} = v_j$, and $\sigma_i \neq \sigma_j$ for any i, j. $T^{\mathrm{c}}_{r_{i,j}} = \sum_{i=1}^{n-1} T^{\mathrm{c}}_{\sigma_i,\sigma_{i+1}}$ denotes the average time required for a classical communication between nodes v_i and v_j through path $r_{i,j}$. Table 1 summarizes the notation adopted through the paper.

[5]The results derived within the paper continue to hold for a different quantum network architecture, given that the relevant parameters are properly set. As instance, it is straightforward to extend the analysis to free-space optical channels by replacing the optical fiber attenuation with the free-space attenuation and the light speed in optical fiber with the light speed in free-space, and by redefining the telecom detector parameters to account for the laser source and BS/PBS characteristics [21].

[6]I.e., a photon with a wavelength assuring low absorption in optical telecom single-mode fibers, hence, facilitating long-distance communications. Specifically, for the considered isotope we have $\lambda_t = 1.476\mu m$.

[7]I.e., two quantum repeaters connected by an optical fiber.

[8]In the following, we assume without loss of generality $T^{\mathrm{c}}_{i,j} = T^{\mathrm{c}}_{j,i}$.

TABLE 1. Adopted notation.

Symbol	Definition
V	set of nodes
E	set of optical links
$d_{i,j}$	length of link $e_{i,j}$
$T^c_{i,j}$	average time for a classical communication between adjacent nodes v_i and v_j
$r_{i,j}$	simple path between nodes v_i and v_j
$T^c_{r_{i,j}}$	average time for a classical communication between nodes v_i and v_j through path $r_{i,j}$
L_0	attenuation length of the optical fiber
p^{ht}	atom-photon entanglement generation probability
τ^p	atom pulse duration
τ^d	duty cycle duration for atom cooling
ν^h/τ^h	herald detector efficiency/duration
ν^t/τ^t	telecom detector efficiency/duration
ν^o/τ^o	optical BSM efficiency/duration
ν^a/τ^a	atomic BSM efficiency/duration
$p = p_i$	atom-photon entanglement generation probability at node v_i
T_i	average time for atom-photon entanglement generation at node v_i
$p_{i,j}$	link entanglement generation probability between adjacent nodes v_i and v_j
$\tau_{i,j}$	time between atom-photon entanglement generation and acks reception at adjacent nodes v_i and v_j
$T^s_{i,j}$	average duration of a successful link entanglement operation between adjacent nodes v_i and v_j
$T^f_{i,j}$	average duration of a failed link entanglement operation between adjacent nodes v_i and v_j
$T_{i,j}$	average time for a link entanglement generation between adjacent nodes v_i and v_j
$p_{r_{i,j}}$	end-to-end entanglement generation probability through route $r_{i,j}$
$\tau_{r_{i,j}}$	average duration of the successful round of link entanglement operations through route $r_{i,j}$
$T_{r_{i,j}}$	average time for an end-to-end entanglement generation through route $r_{i,j}$
T^{ch}	quantum memory coherence time
$\xi_{i,j}(T^{\text{ch}})$	expected link entanglement rate between adjacent nodes v_i and v_j
$\xi_{r_{i,j}}(T^{\text{ch}})$	expected end-to-end entanglement rate between nodes v_i and v_j through route $r_{i,j}$
$r^*_{i,j}$	optimal route between nodes v_i and v_j, i.e., route assuring the highest entanglement rate $\xi_{r^*_{i,j}}(T^{\text{ch}})$

In the following, we gather some definitions.

Definition 1 (Local Entanglement Probability): The *local entanglement generation probability* p_i denotes the probability of successfully generating an atom-photon entanglement at node $v_i \in V$.

Definition 2 (Local Entanglement Time): The *local entanglement generation time* T_i denotes the average time required for successfully generating an atom-photon entanglement at node $v_i \in V$.

Definition 3 (Link Entanglement Probability): The *link entanglement generation probability* $p_{i,j}$ denotes the probability of successfully generating an entanglement between two adjacent nodes v_i and v_j through optical link $e_{i,j}$.

Definition 4 (Link Entanglement Time): The *link entanglement generation time* $T_{i,j}$ denotes the average time required for successfully generating an entanglement between two adjacent nodes v_i and v_j through optical link $e_{i,j}$.

Definition 5 (Link Entanglement Rate): The *link entanglement rate* $\xi_{i,j}(T^{\text{ch}})$ denotes the average number of successful entanglement generations within the unit time between between two adjacent nodes v_i and v_j through optical link $e_{i,j}$, which can be successfully used for teleportation given the quantum memory coherence time T^{ch}.

Definition 6 (End-to-End Entanglement Probability): The *end-to-end entanglement generation probability* $p_{r_{i,j}}$ denotes the probability of successfully generating a remote entanglement between two nodes v_i and v_j through route $r_{i,j}$.

Definition 7 (End-to-End Entanglement Time): The *end-to-end entanglement generation time* $T_{r_{i,j}}$ denotes the average time required for successfully generating a remote entanglement between two nodes v_i and v_j through route $r_{i,j}$.

Definition 8 (End-to-End Entanglement Rate): The *end-to-end entanglement rate* $\xi_{r_{i,j}}(T^{\text{ch}})$ denotes the average number of successful entanglement generations within the unit time between two nodes v_i and v_j through route $r_{i,j}$, which can be successfully used for teleportation given the quantum memory coherence time T^{ch}.

We can now formally define the considered problem.

Optimal Quantum Routing Problem: Given the quantum network $G = (V, E)$ with coherence time T^{ch}, the goal is to choose, for an arbitrary pair source-destination $(v_i, v_j) \in V \times V$, the *optimal route* $r^*_{i,j}$, i.e., the route assuring the highest ent-to-end entanglement rate $\xi_{r^*_{i,j}}(T^{\text{ch}})$ between v_i and v_j.

Remark 2: Two are the main challenges for the considered problem. At first, the complex and stochastic nature of the physical mechanisms underlying quantum entanglement poses significantly challenges in measuring the entanglement rate through an arbitrary path. Furthermore, as we will prove in Section IV-C, the entanglement rate is not isotonic.[9] Hence, traditional routing protocols (such as those based on Dijkstra or Bellman-Ford algorithms) fail in discovering the optimal route, i.e., the route assuring the highest end-to-end entanglement rate, as clearly shown in Section V-B

IV. END-TO-END ENTANGLEMENT RATE

Here, we first analytically derive in Sec. IV-A the closed-form expression of the expected link entanglement rate. Then, we analytically derive in Sec. IV-B the closed-form expression

[9] For a formal definition of isotonicity please refer to Section IV-C

of the expected end-to-end entanglement rate. In Sec. IV-C, we design an optimal routing protocol able to select the route assuring the highest end-to-end entanglement rate between any pair of nodes in any quantum network. Finally, we discuss the derived results in Section IV-D.

A. LINK ENTANGLEMENT

First, we observe that the local entanglement generation probability p_i at node i is affected by two main factors [20]:

i) successful generation of a herald photon and a telecom photon, assumed constant at each node since influenced by the isotope unwanted initial-states and decay-paths;
ii) the parasitic losses in the heralding and entangling cavity, assumed constant at each node since influenced by the detector technology.

Hence, p_i can be written as:

$$p_i = \left(p^{ht} \nu^h \nu^t\right) \tag{1}$$

with p^{ht} denoting the photons generation probability, and ν^h and ν^t denoting the heralding and entangling detector efficiency, respectively. In the following, without loss of generality, we will omit the i-th node dependence from p_i for the sake of notation simplicity, i.e., $p_i = p \; \forall v_i \in V$.

Once a heralded local entanglement is generated at each node, the two photons must be sent to the BSM and must be measured, as shown in Figure 2. Hence, by accounting for (1), the link entanglement generation probability $p_{i,j}$ is equal to [20]:

$$p_{i,j} = \frac{1}{2}\nu^o \left(p e^{-d_{i,j}/(2L_0)}\right)^2 = \frac{1}{2}\nu^o p^2 e^{-d_{i,j}/L_0} \tag{2}$$

where ν^o denotes the optical BSM efficiency (assumed constant at each node), $d_{i,j}$ denotes the length of link $e_{i,j}$, L_0 denotes the attenuation length of the optical fiber, and the term $\frac{1}{2}$ accounts for the optical BSM capability of unambiguously identifying only two out of four Bell states.

The average time T_i required for a single atom-photon entanglement operation is equal to:

$$T_i = \tau^p + \max\{\tau^h, \tau^t\} \quad \forall v_i \in V \tag{3}$$

with τ^p denoting the duration of the pulse required to excite the atom, and τ^h and τ^t denoting the time expectation for heralding-cavity and telecom-cavity output (again, assumed constant at each node without loss of generality).

Once an atom-photon entanglement operation is performed, the two photons must be sent to the optical BSM, and then an acknowledgment of the arrival of the photons must be sent back from the BSM to each node.[10] If the first link entanglement attempt succeeds, the average time $T^s_{i,j}$ required for the successful attempt is equal to:

$$T^s_{i,j} = \tau^p + \max\left\{\tau^h, \tau_{i,j}\right\} \tag{4}$$

[10]The acks can be sent through full-duplex optical links with classical communications characterized by a negligible error rate .

where the average time $\tau_{i,j}$ elapsed between the atom-photon entanglement generation and the ack reception is given by:

$$\tau_{i,j} = \tau^t + \frac{d_{i,j}}{2c_f} + \tau^o + T^c_{i,j} \tag{5}$$

with c_f denoting the light speed in optical fiber, τ^o denoting the time required for the optical BSM, and $T^c_{i,j}$ denoting the time required for ack transmission over classical communication link between nodes v_i and v_j. Otherwise, if the first attempt fails, an additional time τ^d is required for cooling the atom before to start a new local entanglement generation, and the total average time $T^f_{i,j}$ required for the failed attempt is equal to:

$$T^f_{i,j} = \tau^p + \max\left\{\tau^h, \tau_{i,j}, \tau^d\right\} \tag{6}$$

By accounting for (2) and (6), we derive in Lemma 1 the average time $T_{i,j}$ for a link entanglement generation

Lemma 1 (Link Entanglement Generation Time): The average time required to generate a remote entanglement between two adjacent nodes v_i and v_j is equal to:

$$T_{i,j} = \frac{\bar{p}_{i,j} T^f_{i,j} + p_{i,j} T^s_{i,j}}{p_{i,j}} \tag{7}$$

with $\bar{p}_{i,j} \stackrel{\triangle}{=} 1 - p_{i,j}$ and $T^f_{i,j}$ and $T^s_{i,j}$ given in (4) *and* (6)*, respectively.*

Proof: See Appendix A. ■

Stemming from Lemma 1, the link entanglement rate $\xi_{i,j}(T^{\text{ch}})$ is derived in Theorem 1.

Theorem 1 (Link Entanglement Rate): The expected entanglement rate $\xi_{i,j}(T^{ch})$ between adjacent nodes v_i and v_j is equal to:

$$\xi_{i,j}(T^{ch}) = \begin{cases} 0 & \text{if } T^{ch} < \tau_{i,j} \\ 1/T_{i,j} & \text{otherwise} \end{cases} \tag{8}$$

with T^{ch} denoting the quantum memory coherence time and $\tau_{i,j}$ given in (5).

Proof: See Appendix B. ■

Remark 3: From (5), $\tau_{i,j}$ denotes the average time elapsed between: i) the atom-photon entanglement generations at the adjacent nodes v_i and v_j, and ii) the receptions of the entanglement acks at the same nodes through classical communications. Since the degradation of the qubit stored at each adjacent node starts at the emission of the telecom-wavelength photon during the local entanglement operation, $\tau_{i,j}$ represents the minimum storing time required to the quantum memories for successfully utilizing a link entanglement.

B. END-TO-END ENTANGLEMENT

Once an entanglement between adjacent nodes is obtained, remote entanglement between non-adjacent nodes can be generated by performing entanglement swapping at intermediate nodes through atomic BSM.

By denoting with τ^a and ν^a the duration and the efficiency of a single atomic BSM, respectively, we derive in

Lemma 2 the average time for an end-to-end entanglement generation $T_{r_{i,j}}$.

Lemma 2 (End-to-End Entanglement Generation Time): The expected time required to generate a remote entanglement between two non-adjacent nodes v_i and v_j through route $r_{i,j}$ is given by:

$$T_{r_{i,j}} = T_{r_{\sigma_1,\sigma_n}} \tag{9}$$

with $T_{r_{\sigma_l,\sigma_m}}$ for the arbitrary sub-route r_{σ_l,σ_m} recursively defined as in (10) *shown at the bottom of this page, and with $T^c_{r_{\sigma_l,\sigma_m}} = \sum_l^{m-1} T^c_{\sigma_l,\sigma_{l+1}}$.*

Proof: *See Appendix C.* ■

Stemming from Lemma 2, the end-to-end entanglement rate $\xi_{r_{i,j}}(T^{\text{ch}})$ is derived in Theorem 2.

Theorem 2 (End-to-End Entanglement Rate): The expected entanglement rate $\xi_{r_{i,j}}(T^{ch})$ between nodes v_i and v_j through route $r_{i,j}$ is equal to:

$$\xi_{r_{i,j}}(T^{ch}) = \begin{cases} 0 & \text{if } T^{ch} < \tau_{r_{i,j}} - \min\limits_{l=1,n-1} \left\{ T^s_{\sigma_l,\sigma_{l+1}} - \tau_{\sigma_l,\sigma_{l+1}} \right\} \\ \frac{1}{T_{r_{i,j}}} & \text{otherwise} \end{cases} \tag{11}$$

with T^{ch} denoting the quantum memory coherence time and $\tau_{r_{\sigma_l,\sigma_m}}$ recursively defined as in (12) *shown at the bottom of this page.*

Proof: *See Appendix D.* ■

Remark 4: $\tau_{r_{\sigma_l,\sigma_m}}$ given in (12) denotes average duration of the successful (last) round of link entanglement operations required to generate a remote entanglement between two non-adjacent nodes v_i and v_j through route $r_{i,j}$.

Remark 5: It is straightforward to prove that, under the reasonable assumption of BSM duration and efficiency constant at each node, by maximizing the entanglement rate $\xi_r(T^{\text{CH}})$ we are maximizing the teleportation rate as well.

Stemming from Theorem 2, Algorithm 1 provides the pseudo-code for computing the expected entanglement rate $\xi_{r_{i,j}}(T^{\text{ch}})$ between nodes v_i and v_j through route $r_{i,j}$, whereas Algorithm 2 describes two auxiliary functions. Specifically, at first Algorithm 1 computes the link entanglement generation time $T_{l,m}$ for any link $e_{l,m}$ composing path $r_{i,j}$ (lines 4-11), in agreement with (7). Then, if path $r_{i,j}$ is composed by a single link (lines 13-16) and the time $\tau_{l,m}$ elapsed since the entanglement generation is smaller than than the quantum memory coherence time T^{ch} (line 14), the entanglement rate $\xi_{r_{i,j}}(T^{\text{ch}})$ is obtained as the reciprocal of the link entanglement generation time $T_{l,m}$ (line 15), in agreement with (8). Differently, if path $r_{i,j}$ is composed by multiple links (lines 17-31), route $r_{i,j}$ is split into two sub-routes $r_{i,k}$ and $r_{k,j}$ at intermediate node v_k (line 18). Then, the entanglement generation times $T_{r_{i,k}}$ and $T_{r_{k,j}}$ are recursively computed (lines 19-20) through function recT$(\cdot)$ given in Algorithm 2, in agreement with (10). Finally, if the time

Algorithm 1 Expected Entanglement Rate

1: // $D = \{d_{l,m} : e_{l,m} \in E\}$, $T^{\text{c}} = \{T^{\text{c}}_{l,m} : e_{l,m} \in E\}$
2: // $T^s = \{T^s_{l,m} : e_{l,m} \in E\}$, $T = \{T_{l,m} : e_{l,m} \in E\}$
3: **function** Xi($r_{i,j}$, D)
4:   **for** link $e_{l,m} \in r_{i,j}$ **do**
5:     $p_{l,m} = \frac{1}{2} \nu_o p^2 e^{-d_{l,m}/L_0}$
6:     $T^{\text{c}}_{l,m} = d_{l,m}/(2c_f)$
7:     $\tau_{l,m} = \tau^t + \tau^o + d_{l,m}/(2c_f) + T^{\text{c}}_{l,m}$
8:     $T^s_{l,m} = \tau^p + \max\{\tau^h, \tau_{l,m}\}$
9:     $T^f_{l,m} = \tau^p + \max\{\tau^h, \tau_{l,m}, \tau^d\}$
10:     $T_{l,m} = \left((1 - p_{l,m})T^f_{l,m} + p_{l,m}T^s_{l,m}\right)/p_{l,m}$
11:   **end for**
12:   $n = \text{numLinks}(r_{i,j})$
13:   **if** $n = 1$ **then**
14:     **if** $\tau_{l,m} \le T^{CH}$ **then**
15:       $\xi_{r_{i,j}} = 1/T_{l,m}$
16:     **end if**
17:   **else**
18:     $k = \lceil (n+1)/2 \rceil$
19:     $T_{r_{i,k}} = \text{recT}(r_{i,k}, T, T^{\text{c}})$
20:     $T_{r_{k,j}} = \text{recT}(r_{k,j}, T, T^{\text{c}})$
21:     $\tilde{T} = \max\{T_{r_{i,k}}, T_{r_{k,j}}\}$
22:     $\tilde{T}^{\text{c}} = \max\{T^{\text{c}}_{r_{i,k}}, T^{\text{c}}_{r_{k,j}}\}$ // $T^{\text{c}}_{r_{i,k}} = \sum_{e_{l,m} \in r_{i,k}} T^{\text{c}}_{l,m}$
23:     $T_{r_{i,j}} = \left(\tilde{T} + \tau^a + \tilde{T}^{\text{c}}\right)/\nu^a$
24:     $\tau_{r_{i,k}} = \text{recTau}(r_{i,k}, T^s, T^{\text{c}})$
25:     $\tau_{r_{k,j}} = \text{recTau}(r_{k,j}, T^s, T^{\text{c}})$
26:     $\tilde{\tau} = \max\{\tau_{r_{i,k}}, \tau_{r_{k,j}}\}$
27:     $\tau_{r_{i,j}} = \tilde{\tau} + \tau^a + \tilde{T}^{\text{c}}$
28:     **if** $\tau_{r_{i,j}} - \min\limits_{e_{l,m} \in r_{i,j}} \{T^s_{l,m} - \tau_{l,m}\} \le T^{CH}$ **then**
29:       $\xi_{r_{i,j}} = 1/T_{r_{i,j}}$
30:     **end if**
31:   **end if**
32:   **return** $\xi_{r_{i,j}}$
33: **end function**

$$T_{r_{\sigma_l,\sigma_m}} = \begin{cases} \left(\max\left\{T_{r_{\sigma_l,\sigma_k}}, T_{r_{\sigma_k,\sigma_m}}\right\} + \tau^a + \max\left\{T^{\text{c}}_{r_{\sigma_l,\sigma_k}}, T^{\text{c}}_{r_{\sigma_k,\sigma_m}}\right\}\right)/\nu^a, \quad k = \left\lceil \frac{m+l}{2} \right\rceil & \text{if } m > l+1 \\ T_{\sigma_l,\sigma_{l+1}} & \text{otherwise} \end{cases} \tag{10}$$

$$\tau_{r_{\sigma_l,\sigma_m}} = \begin{cases} \max\left\{\tau_{r_{\sigma_l,\sigma_k}}, \tau_{r_{\sigma_k,\sigma_m}}\right\} + \tau^a + \max\left\{T^{\text{c}}_{r_{\sigma_l,\sigma_k}}, T^{\text{c}}_{r_{\sigma_k,\sigma_m}}\right\}, \quad k = \left\lceil \frac{m+l}{2} \right\rceil & \text{if } m > l+1 \\ T^s_{\sigma_l,\sigma_{l+1}} & \text{otherwise} \end{cases} \tag{12}$$

Algorithm 2 Auxiliary Functions

1: **function** recT($r_{a,b}, T, T^{\mathrm{c}}$)
2: $n = \text{numLinks}(r_{a,b})$
3: **if** $n = 1$ **then**
4: $T_{r_{a,b}} = T_{a,b}$ // $T = \{T_{l,m} : e_{l,m} \in E\}$
5: **else**
6: $k = \lceil (a+b)/2 \rceil$
7: $T_{r_{a,k}} = \text{recT}(r_{a,k}, T, T^{\mathrm{c}})$
8: $T_{r_{k,b}} = \text{recT}(r_{k,b}, T, T^{\mathrm{c}})$
9: $\tilde{T} = \max\{T_{r_{a,k}}, T_{r_{k,b}}\}$
10: $\tilde{T}^{\mathrm{c}} = \max\{T^{\mathrm{c}}_{r_{a,k}}, T^{\mathrm{c}}_{r_{k,b}}\}$ // $T^{\mathrm{c}}_{r_{a,k}} = \sum_{e_{l,m} \in r_{a,k}} T^{\mathrm{c}}_{l,m}$
11: $T_{r_{i,j}} = \left(\tilde{T} + \tau^a + \tilde{T}^{\mathrm{c}}\right) / \nu^a$
12: **end if**
13: **end function**

14: **function** recTau($r_{a,b}, T^s, T^{\mathrm{c}}$)
15: $n = \text{numLinks}(r_{a,b})$
16: **if** $n = 1$ **then**
17: $\tau_{r_{a,b}} = T^s_{a,b}$ // $T^s = \{T^s_{l,m} : e_{l,m} \in E\}$
18: **else**
19: $k = \lceil (a+b)/2 \rceil$
20: $\tau_{r_{a,k}} = \text{recTau}(r_{a,k}, T^s, T^{\mathrm{c}})$
21: $\tau_{r_{k,b}} = \text{recTau}(r_{k,b}, T^s, T^{\mathrm{c}})$
22: $\tilde{\tau} = \max\{\tau_{r_{a,k}}, \tau_{r_{k,b}}\}$
23: $\tilde{T}^{\mathrm{c}} = \max\{T^{\mathrm{c}}_{r_{a,k}}, T^{\mathrm{c}}_{r_{k,b}}\}$ // $T^{\mathrm{c}}_{r_{a,k}} = \sum_{e_{l,m} \in r_{a,k}} T^{\mathrm{c}}_{l,m}$
24: $\tau_{r_{a,b}} = \tilde{\tau} + \tau^a + \tilde{T}^{\mathrm{c}}$
25: **end if**
26: **end function**

$\tau_{r_{i,j}} - \min\{T^s_{l,m} - \tau_{l,m}\}$ elapsed since the oldest entanglement generation is smaller than the quantum memory coherence time T^{ch} (line 28), the entanglement rate $\xi_{r_{i,j}}(T^{\mathrm{ch}})$ is obtained as the reciprocal of the end-to-end entanglement generation time $T_{r_{i,j}}$ (line 29), in agreement with (11). We note the computation of $\tau_{r_{i,k}}$ and $\tau_{r_{j,k}}$ represents the preliminary step for obtaining $\tau_{r_{i,j}}$ (lines 26-27), and both $\tau_{r_{i,k}}$ and $\tau_{r_{j,k}}$ are recursively computed (lines 29-24) through function recTau($\cdot$) given in Algorithm 2, in agreement with (12).

Corollary 1 (Algorithm 1 Complexity): Algorithm 1 exhibits a linearithmic time complexity $\mathcal{O}(n \log n)$ with the number n of links belonging to the route:

Proof: See Appendix E. ■

C. OPTIMAL QUANTUM ROUTING

Here, we design an optimal routing protocol for quantum networks based on the expected end-to-end entanglement rate $\xi_{r_{i,j}}(T^{\mathrm{ch}})$. To this aim, the following preliminaries are needed.

Definition 9 (Optimality): A route metric is defined *optimal* if there exists a routing protocol that, when used in conjunction with such a metric, always discovers the most favorable path between any pair of nodes in any connected network.

Remark 6: It has been widely recognized in classical-networks literature [26]–[29] that the lack of the optimality property is not trivial: the packets can be routed either through sub-optimal routes, wasting the network resources, or even worse through route loops, causing unreachable destinations. Clearly, these issues become more severe in quantum networks, due to the intrinsic difficulties imposed by entanglement generation and the limits imposed by the no-copying theorem.

Definition 10 (Strict Monotonicity): A routing metric $W : R \longrightarrow \mathbb{R}$ is strictly monotone if and only if:

$$W(r_{i,j}) > W(r_{i,j} \oplus e_{j,k}) \quad \forall\, r_{i,j} \in R, e_{j,k} \in E \tag{13}$$

with R denoting the set of simple paths in the arbitrary network, $\oplus$ is the operator that concatenates a simple path with a link, and $>$ denoting the ordering relation over the paths, i.e., the higher is the entanglement rate, the more preferable is the path.

Remark 7: Clearly, the order relation over the paths depends on the routing metric, with $>$ adopted with metrics modeling an opportunity (as in our case) and $<$ adopted with metrics modeling a cost.

Definition 11 (Strict Isotonicity): A routing metric $W : R \longrightarrow \mathbb{R}$ is strictly isotone if and only if:

$$W(r_{i,j}) < W(\tilde{r}_{i,j}) \Longrightarrow W(r_{i,j} \oplus e_{j,k}) < W(\tilde{r}_{i,j} \oplus e_{j,k}) \tag{14}$$

for any $r_{i,j}, \tilde{r}_{i,j} \in R$ and $e_{j,k} \in E$.

Remark 8: A brief discussion about the importance of the monotonicity and the isotonicity properties is provided in Appendix F and Appendix G, respectively.

Lemma 3 (Monotonicity): The route metric

$$W(r_{i,j}) \stackrel{\triangle}{=} \xi_{r_{i,j}}(T^{CH}) \quad \forall\, r_{i,j} \in R \tag{15}$$

based on the end-to-end entanglement rate given in (11) *is strictly monotone for any route $r_{i,j}$.*

Proof: See Appendix H. ■

Remark 9: We note that $W(r_{i,j})$ given in (15) is strictly monotone for any realistic parameter setting, i.e., $\nu^a < 1$ and $\tau^a > 0$. Nevertheless, even under the unrealistic assumption of $\nu^a = 1$ and $\tau^a = 0$, $W(r) = \xi_r(T^{\mathrm{CH}})$ is still monotone, i.e., $W(r) \geq W(r \oplus e)\ \forall\, r \in R, e \in E$, and the results derived in the subsequent theorem continue to hold.

Lemma 4 (Strict Isotonicity): The route metric $W(r_{i,j})$ given in (15) *is not strictly isotone.*

Proof: See Appendix I. ■

Stemming from Lemmas 3-4, Algorithm 3 provides the pseudo-code for the optimal routing protocol, i.e., the protocol able to always converges to the optimal route $r^*_{i,j}$ between any pair of nodes v_i and v_j in any connected quantum network. Specifically, Algorithm 3 implements a simple path enumeration algorithm adapted from [30]. At first (lines 4-9), the algorithm generates all the routes with no internal vertices (i.e., the simple paths composed by a single link), and it computes the entanglement rate along such routes through function Xi($\cdot$) given in Algorithm 1 (line 8). Then (lines 10-25), the algorithm concatenates two sub-simple-paths p_1 and p_2 between vertices v_i-v_k and v_k-v_j,

Algorithm 3 Optimal Path Selection

1: // $D = \{d_{i,j}\}_{e_{i,j} \in E}$
2: **function** optimalPath(V, E, D)
3:     $w_{i,j} = 0 \; \forall \, v_i, v_j \in V$
4:     **for** link $e_{i,j} \in E$ **do**
5:         $R(i,j).append(e_{i,j})$
6:         $r^*_{i,j} = e_{i,j}$
7:         // Xi($\cdot$) defined in Algorithm 1
8:         $w_{i,j} = \text{Xi}(e_{i,j}, D)$
9:     **end for**
10:     **for** $v_k \in V$ **do**
11:         **for** $v_i \in V$ **do**
12:             **for** $v_j \in V$ **do**
13:                 **for** path $p_1 \in R(i,k)$ and $p_2 \in R(k,j)$ **do**
14:                     **if** $!(V(p_1) \;\&\; V(p_2) \;\&\; V \setminus \{k\})$ **then**
15:                         $r = p_1 \oplus p2$
16:                         $R(i,j).append(r)$
17:                         **if** Xi(r, D) $> w_{i,j}$ **then**
18:                             $r^*_{i,j} = r$
19:                             $w_{i,j} = \text{Xi}(r, D)$
20:                         **end if**
21:                     **end if**
22:                 **end for**
23:             **end for**
24:         **end for**
25:     **end for**
26:     **return** $\{r^*_{i,j}, w_{i,j}\}_{v_i, v_j \in V}$
27: **end function**

respectively, given that the resulting path $r = p_1 \oplus p_2$ between vertices v_i and v_j is simple, i.e., given that the intersection of the vertices $V(p_1)$ of path p_1 with the vertices $V(p_2)$ of path p_2 is empty with the exception of vertex v_k (line 14). The entanglement rate along the concatenated path $r = p_1 \oplus p_2$ is computed through function Xi($\cdot$) given in Algorithm 1 (line 17), and the optimal path $r^*_{i,j}$ between vertices v_i and v_j is updated depending on the computed entanglement rate (lines 17-20).

Theorem 3 (Optimality): The route metric $W(r_{i,j})$ given in (15) *is optimal for any source-destination pair v_i, v_j when combined with the routing protocol given in Algorithm 3.*

Proof: See Appendix J. ■

Corollary 2 (Non Optimality): The route metric $W(r_{i,j})$ given in (15) *is not optimal when combined with any routing protocol based on Dijkstra or Bellman-Ford algorithms.*

Proof: It follows by reasoning as in Appendix J. ■

Corollary 3 (Algorithm 3 Complexity): Algorithm 3 exhibits a time complexity equal to $\mathcal{O}(|V|^3|S||E| \log |E|)$, polynomial with the number $|V|$ of vertices, linearithmic with the number $|E|$ of edges and linear with the number $|S|$ of simple routes in G.

Proof: See Appendix K. ■

D. DISCUSSION

Here we conduct a brief discussion stemming from the results derived through the paper.

The implicit assumption of our theoretical analysis is that the local entanglements start simultaneously, i.e., the swapping strategy is not optimized with respect to the times $\{T_{i,j}\}$. As instance, let us consider the route $r_{1,4}$ shown in Figure 4 by assuming $T^s_{1,2} = T^s_{2,3} >> T^s_{3,4}$. If we neglect the decoherence effects, the two swapping strategies shown in figure are equivalent. Differently, if we aim at minimizing the decoherence effects, it would be better to adopt strategy *i*) and to delay the link entanglement generation at $e_{3,4}$ as much as possible. We leave the analysis of the swapping strategy optimization as a future work.

Furthermore, we explicitly neglect the effects of entanglement purification in our rate analysis. The rationale for this choice is that the adopted quantum repeater architecture is characterized by an extremely high fidelity, with values close to $F = 0.99$ [20], [31]. Nevertheless, we plan to incorporate the purification mechanism within the end-to-end entanglement rate analysis in a future work.

Finally, from Corollary 3, we observe that the time complexity of the proposed routing procedure depends on the number of simple paths through the function optimalPath($\cdot$). This constitutes a scalability issue in large or full-connected quantum networks, where S grows factorially in $|V|$. However, it seems unreasonable to expect such quantum topologies due to the quantum technology costs and the exponential decay of communication rate as a function of the distance. In any case, the factorial complexity in $|V|$ can be easily scaled down to a polynomial complexity by exploiting zone-based routing or routing based on near-optimal evolutionary algorithms [32], [33]. We plan to study this issue in a future work.

V. NUMERICAL RESULTS

A. ENTANGLEMENT RATE

Here, we evaluate both the link and the end-to-end entanglement rate by adopting the quantum repeater model shown in Figure 2.

All the parameters have been set in agreement with experimental results [20], [23], but we note that the analytical results derived in Sec. IV continue to hold for any different parameter setting.

Specifically, we set $p^{ht} = 0.53$, $\nu^h = \nu^t = 0.8$, $\nu^a = 0.3904$, $L_0 = 22km$, $c_f = 2 * 10^8 m/s$, $\tau^p = 5.9\mu s$, $\tau^h = 20\mu s$, $\tau^t = 10\mu s$ and $\tau^d = 100\mu s$. Furthermore, we set $T^c_{i,j} = d_{i,j}/(2c_f)$ by neglecting the delay introduced by the optical amplifiers, and we set $\tau^o = \tau^a = 10\mu s$ analogously[11] to τ^t and $\nu^a = 0.39$ analogously to ν^o. Finally, we reasonably assume quantum memories with coherence time $T^{ch} = 10ms$, since coherence times greater than ten seconds have

[11] The analytical results derived in Sec. IV continue to hold for any different time-parameters setting.

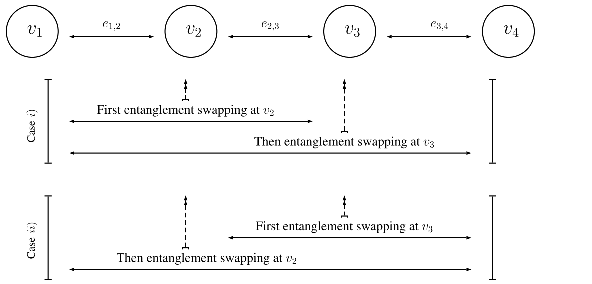

FIGURE 3. Swapping strategy alternatives: case i) first entanglement swapping at v_2 and then at v_3; case ii) first entanglement swapping at v_3 and then at v_2.

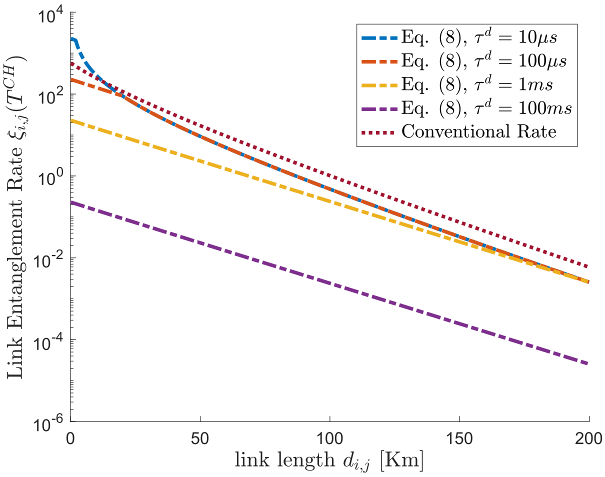

FIGURE 4. Expected Link Entanglement Rate $\xi_{i,j}(T^{ch})$ between adjacent nodes v_i and v_j as a function of the optical link length $d_{i,j}$ for different values of the time τ^d required for atom cooling. Decoherence time T^{ch} equal to 10*ms*. Logarithmic scale for *y* axis.

been already reported for the adopted qubit implementation (i.e., ^{87}Rb) [34].

In Figure 4, we show the expected link entanglement rate $\xi_{i,j}(T^{\text{ch}})$ between adjacent nodes v_i and v_j given in (8) as a function of the optical link length $d_{i,j}$ for different values of the time τ^d required for atom cooling (ranging from $10\mu s$ to $0.1s$). For performance comparison, we consider the approximation of the link entanglement rate recently proposed in [20], referred to as *Conventional Rate* and approximating the rate as $p_{i,j}/(d_{i,j}/c_f + \tau)$ with $\tau = 100\mu s$ and $\nu^o = 1$ (i.e., ideal optical BSM). First, we note that the approximation slightly differs from the exact closed-form expression derived in (8) when $\tau^d = \tau$. Furthermore, we note that the duty cycle duration significantly degrades the achievable rates.

In Figure 5, we show the expected end-end entanglement rate $\xi_{r_{i,j}}(T^{\text{ch}})$ between nodes v_i and v_j through route $r_{i,j}$ given in (11), with $r_{i,j} = \{e_{i,k}, e_{k,j}\}$ constituted by two links. In this experiment, we evaluate the impact of the proportion between the link lengths $d_{i,k}$ and $d_{k,j}$ on the entanglement rate. Furthermore, we also consider the case in which there exists a direct link between v_i and v_j with length $d_{i,j} = d_{i,k} + d_{k,j}$. Finally, for performance comparison, we report the

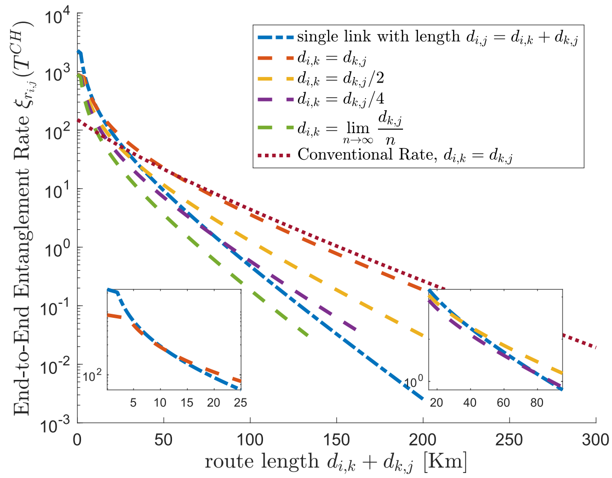

FIGURE 5. Expected End-to-End Entanglement Rate $\xi_{r_{i,j}}(T^{ch})$ between nodes v_i and v_j through route $r_{i,j} = \{e_{i,k}, e_{k,j}\}$ as a function of the total path length $d_{i,k} + d_{k,j}$ for different values of $d_{i,k}$. Atom cooling time τ^d and decoherence time T^{ch} equal to 100μs and 1*ms*, respectively. Logarithmic scale for *y* axis. Subplots highlighting the presence of critical path length for choosing whether to use or not a repeater when: i) the repeater is positioned in the path median (left subplot); ii) the repeater is not positioned in the path median (right subplot).

approximation of the end-to-end entanglement rate recently proposed in [20], referred to as *Conventional Rate*, which is defined only for the case $d_{i,k} = d_{k,j}$. At first, we note that the approximation significantly differs from the exact closed-form expression derived in (8) whenever $d_{i,k} \neq d_{k,j}$, with rates over-estimated by roughly two order of magnitudes. Furthermore, we note that the exact closed-form expression derived in (11) is able to account for the rich dynamic imposed by the ratio of the link lengths. As an example, at $d = 200km$, the end-to-end entanglement rate can vary from 0.19 entanglements/second for $d_{k,j} = d_{i,k}$ to 0 entanglements/second for $d_{k,j} = 4d_{i,k}$ due to the decoherence effects.

The two subplots of Figure 5 highlight the presence of critical path length for choosing whether to use or not a repeater. Specifically, the left subplot focuses on a repeater positioned in the path median, and it shows the presence of a critical path length value so that: i) for paths shorter than such a threshold, connecting v_1 and v_3 with a single link (i.e., without a repeater) with total length equal to $d_{1,2} + d_{2,3}$ assures the highest entanglement rate: ii) on the contrary, for paths longer than such a threshold, connecting v_1 and v_3 through a repeater at v_2 with $d_{1,2} = d_{2,3}$ assures the highest entanglement rate. Clearly, this threshold effect is critical for selecting the shortest-path in complex networks, and it must be carefully taken into account. Similarly, the right subplot shows the presence of a critical path length value even when the repeater is not positioned in the path median.

Finally, in Figure 6, we report the minimum coherence time $\tau_{r_{i,j}}$ required to the quantum memories for the successful utilization of an end-to-end entanglement between nodes v_i and v_j through route $r_{i,j} = \{e_{i,k}, e_{k,j}\}$ for the same simulation set of Figure 5. The analytical expression of $\tau_{r_{i,j}}$ is

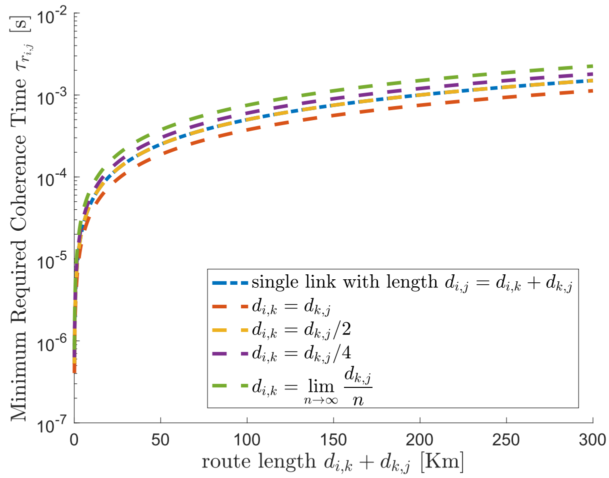

FIGURE 6. Minimum Coherence Time $\tau_{r_{i,j}}$ required for the successful utilization of an end-to-end entanglement between nodes v_i and v_j through route $r_{i,j} = \{e_{i,k}, e_{k,j}\}$ as a function of the total path length $d_{i,k} + d_{k,j}$ for different values of $d_{i,k}$. Atom cooling time τ^d equal to 100μs. Logarithmic scale for y axis.

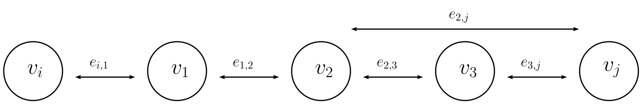

FIGURE 7. Use case: network topology adapted from [27] and [29]. There exist two simple routes from v_i to v_j: i) $r^1_{i,j} = (e_{i,1}, e_{1,2}, e_{2,j})$, ii) $r^2_{i,j} = (e_{i,1}, e_{1,2}, e_{2,3}, e_{3,j})$, resulting from the concatenation of the sub-route $r_{i,2} = (e_{i,1}, e_{1,2})$ with the two routes $r^1_{2,j} = (e_{2,j})$ and $r^2_{2,j} = (e_{2,3}, e_{3,j})$. The length of each link is d, with the exception of link $e_{2,j}$ with length $2d$.

given in (12). We first observe that the minimum coherence times are obtained by using a repeater positioned in the path median. Furthermore, quantum memories with coherence times exceeding the order of ten milliseconds can guarantee an end-to-end entanglement even for the larger values of considered path lengths.

B. ROUTING PROTOCOL OPTIMALITY

Figure 8 shows the expected end-end entanglement rate $\xi_r(T^{\text{ch}})$ for the different routes as a function of the link length d. We note that there exists a critical link length ($d \simeq 5650m$) so that: i) for links shorter than such a threshold, the direct link $r^1_{2,j}$ constitutes the optimal route between v_2 and v_j, whereas ii) for links longer than such a threshold, the path $r^2_{2,j}$ through repeater v_3 constitutes the optimal route between v_2 and v_j. Differently, the path $r^2_{i,j}$ constitutes the optimal route between v_i and v_j for any value of link length. Hence, from the proof of Theorem 3, it follows that any traditional routing protocol based on Dijkstra or Bellman-Ford algorithms would fail in selecting the optimal route $r^2_{i,j}$ for any link-length smaller than the threshold.

To clearly assess the impact of sub-optimality, Figure 9 shows the performance of *optimal* and *sub-optimal* quantum routing for the different routes of Figure 7 as a function of the link length d. Specifically, the figure shows: i) the entanglement rate $\xi_{r^*_{i,j}}$ achievable with the optimal route $r^*_{i,j}$ selected with Algorithm 3, and ii) the entanglement rate $\xi_{r_{i,j}}$ achievable with the route $r_{i,j}$ selected with a routing protocol based on Dijkstra algorithm. We observe that, even for the simple topology of Figure 7, the performance degradation of sub-optimal routing can be severe, with the optimal routing proposed in Algorithm 3 achieving an entanglement rate improvement higher than 250% (for $d = 5650m$, it results $\xi_{r^*_{i,j}}(T^{\text{ch}}) \simeq 93.2$ and $\xi_{r_{i,j}}(T^{\text{ch}}) \simeq 36.3$ entanglements per second, respectively). These results confirm the considerations made in Remarks 2 and 6 about the importance of optimal routing in quantum networks, due to the intrinsic difficulties imposed by entanglement generation and the limits imposed by the no-copying theorem.

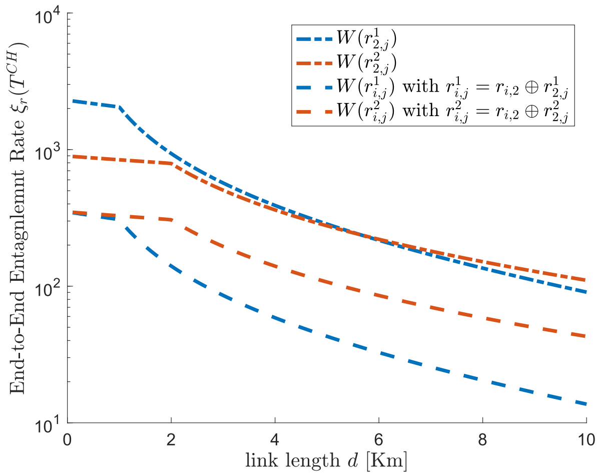

FIGURE 8. Expected End-to-End Entanglement Rate $\xi_r(T^{\text{ch}})$ for the different routes of Figure 7 as a function of the link length d. Atom cooling time τ^d and decoherence time T^{ch} equal to 100μs and 10ms, respectively. Logarithmic scale for y axis.

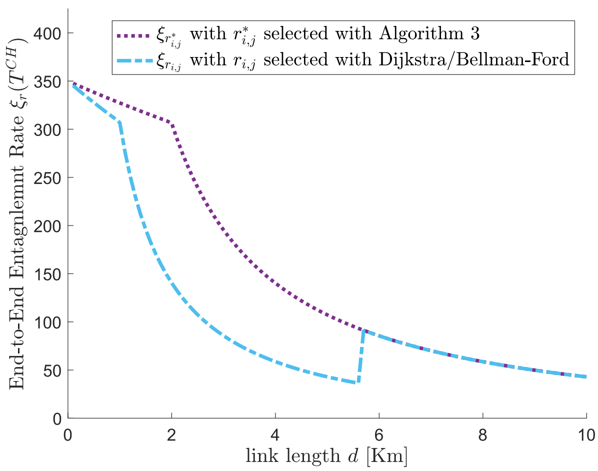

FIGURE 9. Optimal vs Sub-Optimal routing performance in terms of Expected End-to-End Entanglement Rate $\xi_r(T^{\text{ch}})$ for the different routes of Figure 7 as a function of the link length d. Atom cooling time τ^d and decoherence time T^{ch} equal to 100μs and 10ms, respectively.

VI. CONCLUSIONS

In this paper, we designed an *optimal routing protocol* for quantum networks, i.e., a routing protocol that always discovers the route assuring the highest end-to-end entanglement rate between any pair of nodes in any quantum network. To this aim, we first modeled the entanglement generation through a stochastic framework that allowed us to jointly account for all the key physical-mechanisms affecting the end-to-end entanglement rate, such as decoherence time, atom-photon and photon-photon entanglement generation, entanglement swapping and imperfect Bell-state measurement. Then, we derived the closed-form expression of the *end-to-end entanglement rate* for an arbitrary path and we designed an efficient algorithm for entanglement rate computation, exhibiting a linearithmic time complexity. Finally, we designed a routing protocol and we proved its optimality when used in conjunction with a routing metric based on the entanglement rate. Numerical simulations confirmed the superiority of the proposed quantum routing protocol with respect to traditional routing protocols based on Dijkstra or Bellman-Ford algorithms.

APPENDIX

A. PROOF OF LEMMA 1

The thesis follows, after some algebraic manipulations, from the notable relations $\sum_{n=0}^{\infty} nx^n = x/(x-1)^2$ and $\sum_{n=0}^{\infty} x^n = 1/(1-x)$ for $|x| < 1$.

B. PROOF OF THEOREM 1

The thesis follows from (5) and Lemma 1, by noting that:

i) the degradation of the qubit stored at each adjacent node starts at the emission of the telecom-wavelength photon during the local entanglement operation;
ii) every time a link entanglement operation fails, a heralded local entanglement is re-generated at both v_i and v_j;
iii) given that at time $T_{i,j}$ a link entanglement is generated, the most recent emission of telecom-wavelength photons happened at time $T_{i,j} - \tau_{i,j}$, independently from the number of failed link entanglement operations.

C. PROOF OF LEMMA 2

We prove the thesis through mathematical induction.

Basis: Show that the statement hold for when $N = 1$ swapping rounds are required, i.e., when we have a route $r_{i,j} = (e_{i,k}, e_{k,j})$ composed by two links.

To generate a remote entanglement between v_i and v_j, we need first to generate two link entanglements through $e_{i,k}$ and $e_{k,j}$. This operation requires an average time equal to $\max\{T_{i,k}, T_{k,j}\}$. Once done, we have two cases.

i) With probability ν^a an entanglement swapping is generated at node v_k, and the swapping operation requires a time equal to τ^a. Furthermore, an additional time equal to $\max\{T^c_{i,k}, T^c_{k,j}\}$ is required for acknowledging v_i and v_j that a remote entanglement has been successfully generated through classical communication.
ii) With probability $\bar{\nu}^a \triangleq 1 - \nu^a$, the swapping fails in a time equal to τ^a. Furthermore, every time a BSM fails, the link entanglements through $e_{i,k}$ and $e_{k,j}$ must be re-generated. Hence, an additional time equal to $\max\{T^c_{i,k}, T^c_{k,j}\}$ is required for informing v_i and v_j to start a new link entanglement generation process.

Hence, by denoting with $T_{k,k} = \max\{T_{i,k}, T_{k,j}\} + \tau^a + \max\{T^c_{i,k}, T^c_{k,j}\}$ and by accounting for the notable relations $\sum_{n=0}^{\infty} nx^n = x/(x-1)^2$ and $\sum_{n=0}^{\infty} x^n = 1/(1-x)$ when $|x| < 1$, we obtain:

$$T_{i,j} = \sum_{k=0}^{\infty} (k+1) T_{k,k} \left(\bar{\nu}^a\right)^k \nu^a = \frac{T_{k,k}}{\nu^a} \tag{16}$$

and the statement is true for $N = 1$.

Inductive Step: Show that (10) holds for $N+1$ swapping rounds, given that (10) is true for N swapping rounds. We set $r_{i,j} = r_{1,n} = (e_{1,2}, \ldots, e_{n-1,n})$ with n being a power of 2 for the sake of notation simplicity.

To generate an end-to-end entanglement between v_1 and v_n, we need first to generate two end-to-end entanglements between v_1, v_k and v_k, v_n with $k = \left\lceil \frac{n+1}{2} \right\rceil$. This operation requires an average time equal to $\max\{T_{r_{1,k}}, T_{r_{k,n}}\}$. Then, we have two cases.

i) With probability ν^a an entanglement swapping is generated at node v_k in a time equal to τ^a, and v_1 and v_n become aware about the end-to-end entanglement generation through classical communication after an additional time equal to $\max\{T^c_{r_{1,k}}, T^c_{r_{k,n}}\}$.
ii) With probability $\bar{\nu}^a$, the swapping fails in a time equal to τ^a, and an additional time equal to $\max\{T^c_{1k}, T^c_{k,n}\}$ is required to inform each node belonging to the route $r_{1,n}$ that the link entanglements must be re-generated.

Hence, by accounting for the notable relations $\sum_{n=0}^{\infty} nx^n = x/(x-1)^2$ and $\sum_{n=0}^{\infty} x^n = 1/(1-x)$ when $|x| < 1$, the thesis follows.

D. PROOF OF THEOREM 2

First, we note that:

i) the degradation of the qubit stored at each adjacent node starts at the emission of the telecom-wavelength photon during the local entanglement operation;
ii) every time an entanglement swapping operation fails, a link entanglement is re-generated at each edge $e_{\sigma_i,\sigma_{i+1}} \in r_{i,j}$ composing the route;
iii) given that at time $T_{r_{i,j}}$ an end-to-end entanglement is generated, the most recent round of link entanglement operations started at time $T_{r_{i,j}} - \tau_{r_{i,j}}$ (with $\tau_{r_{i,j}}$ derived in (12) by accounting for Lemma 2), independently from the number of failed link entanglement rounds;
iv) given that at time $T_{r_{i,j}} - \tau_{r_{i,j}}$ the most recent round of link entanglement operations started, the subsequent emission of telecom-wavelength photons for link $e_{\sigma_l,\sigma_{l+1}}$ happened at time $T_{r_{i,j}} - \left(\tau_{r_{i,j}} - (T^s_{\sigma_l,\sigma_{l+1}} - \tau_{\sigma_l,\sigma_{l+1}})\right)$.

E. PROOF OF COROLLARY 1

Given that route $r_{i,j}$ is composed by n links, Algorithm 1 requires $\mathcal{O}(n)$ operations for lines 2-9, 20 and 26 each, two calls to auxiliary function RecT$(\cdot)$ and two calls to function RecTau$(\cdot)$ in lines 17-18 and 22-23, and a constant number of operations in the remaining lines. Each call operates on a route composed at most by $n/2$ links, requiring two recursive calls on a route composed at most by $n/4$ links plus $(O)(n/2)$ operations.

Hence, by denoting with $T(n)$ the time required to execute Algorithm 1 and by denoting $\mathcal{O}(n)$ as n, we have:

$$\begin{aligned} T(n) &= 4T(n/2) + n = 4\left[2T(n/4) + n/2\right] + n = \\ &= 8T(n/4) + 3n = 8\left[2T(n/8) + n/4\right] + 3n = \\ &= 16T(n/8) + 5n = \ldots = 2^{k+1}T(n/2^k) + (2k-1)n \\ &= 2^{\log_2 n+1}T(1) + 2n\log_2 n \end{aligned} \tag{17}$$

By noting that, when the route is composed by one link, each auxiliary function requires a fixed number of operations, we have the thesis.

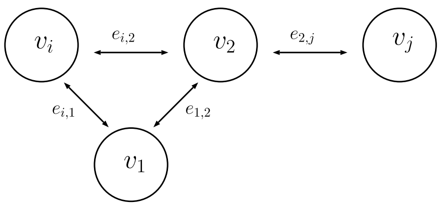

FIGURE 10. Example topology to show the importance of monotonicity property.

F. MONOTONICITY PROPERTY

We illustrate the importance of the monotonicity property through the simple example proposed in [27] and depicted in Figure 10. We assume that the routing metric $W(\cdot)$ (modeling an opportunity, i.e., the higher $W(\cdot)$ the better) is not monotone, i.e., $W(e_{i,1}) < W(e_{i,1} \oplus e_{1,2})$. Additionally, we suppose:

$$W(e_{i,1} \oplus e_{1,2}) > W(e_{i,2}) > W(e_{i,1}) \tag{18}$$

$$W(e_{i,1} \oplus e_{1,2} \oplus e_{2,j}) > W(e_{i,2} \oplus e_{2,j}) \tag{19}$$

Any routing protocol based on Dijkstra or Bellman-Ford algorithms used in conjunction with the defined metric $W(\cdot)$ would fail in finding the optimal route from v_i to v_j. Indeed, both v_1 and v_2 are candidate vertices to forward the packets from v_i to v_j, with v_1 being the optimal forwarder from (18). However, since $W(e_{i,2}) > W(e_{i,1})$, node v_2 is considered by Dijkstra algorithm before node v_1. Hence, the algorithm selects $e_{i,2} \oplus e_{2,j}$ as path toward v_j and this choice remains unchanged. From (19), it is easy to see that Dijkstra's algorithm in conjunction with $W(\cdot)$ fails in finding the optimal route.

G. ISOTONICITY PROPERTY

We illustrate the importance of the isotonicity property through the simple example proposed in [27] and depicted in Figure 11. We assume that the routing metric $W(\cdot)$ (modeling an opportunity, i.e., the higher $W(\cdot)$ the better) is not isotone, i.e., $W(e_{i,1}) > W(\tilde{e}_{i,1})$ and $W(e_{i,1} \oplus e_{1,j}) < W(\tilde{e}_{i,1} \oplus e_{1,j})$.

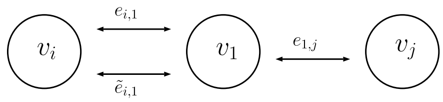

FIGURE 11. Example topology to show the importance of isotonicity property.

Any routing protocol based on Dijkstra or Bellman-Ford algorithms used in conjunction with the defined metric $W(\cdot)$ would fail in finding the optimal route from v_i to v_j. Indeed, both $e_{i,1}$ and $\tilde{e}_{i,1}$ are candidate links to forward the packets from v_i to v_j, with $\tilde{e}_{i,1}$ being the optimal choice since $W(e_{i,1} \oplus e_{1,j}) < W(\tilde{e}_{i,1} \oplus e_{1,j})$. However, since $W(e_{i,1}) > W(\tilde{e}_{i,1})$, when Dijkstra algorithm considers v_1, the algorithm selects $e_{i,1} \oplus e_{1,j}$ as path toward v_j and this choice remains unchanged. Hence, Dijkstra's algorithm in conjunction with $W(\cdot)$ fails in finding the optimal route.

H. PROOF OF LEMMA 3

We prove the case with a *reductio ad absurdum* by supposing that it exist $r_{i,j} \in R$ and $e_{j,k} \in E$ so that $W(r_{i,j}) = W(r_{i,j} \oplus e_{j,k})$. Let us assume $r_{i,j} = r$ composed by n links, with n being a power of 2, and $e_{j,k} = e$ for the sake of notation simplicity.

From (10), we have:

$$T_{r\oplus e} = \frac{\max\{T_r, T_e\} + \tau^a + \max\left\{T_r^c, T_e^c\right\}}{\nu^a} \geq T_r \tag{20}$$

since $\nu^a \leq 1$ and $\tau^a > 0$. Similarly, from (12), we have:

$$\tau_{r\oplus e} = \max\left\{\tau_r, T_e^s\right\} + \tau^a + \max\left\{T_r^c, T_e^c\right\} \geq \tau_r \tag{21}$$

being τ^a and T_r^c, T_e^c not null. By accounting for (20) and (21) and by noting that:

$$\min_{r\oplus e}\left\{T^s_{\sigma_l,\sigma_{l+1}} - \tau_{\sigma_l,\sigma_{l+1}}\right\} \leq \min_r\left\{T^s_{\sigma_l,\sigma_{l+1}} - \tau_{\sigma_l,\sigma_{l+1}}\right\} \tag{22}$$

from (11), we obtain:

$$W(r \oplus e) = \xi_{r\oplus e} < \xi_r = W(r) \tag{23}$$

and (23) constitutes a *reductio ad absurdum*.

I. PROOF OF LEMMA 4

We prove the case with a *reductio ad absurdum* by supposing that

$$W(r_{i,j}) < W(\tilde{r}_{i,j}) \Longrightarrow W(r_{i,j} \oplus e_{j,k}) < W(\tilde{r}_{i,j} \oplus e_{j,k}) \tag{24}$$

for any $r_{i,j}, \tilde{r}_{i,j} \in R$ and $e_{j,k} \in E$. Let us assume both $r_{i,j} = r$ and $\tilde{r}_{i,j} = \tilde{r}$ composed by n links, with n being a power of 2, and $e_{j,k} = e$ for the sake of notation simplicity. Furthermore, we assume without loss of generality $T_e > \max\{T_r, T_{\tilde{r}}\}$ and $T_e^c > \max\{T_r^c, T_{\tilde{r}}^c\}$. From (10), it results:

$$T_{r\oplus e} = \frac{T_e + \tau^a + T_e^c}{\nu^a} = T_{\tilde{r}\oplus e} \tag{25}$$

Hence, whenever $T^{\mathrm{CH}} > \max\{T_{r\oplus e}, T_{\tilde{r}\oplus e}\}$, from (11) we obtain:

$$W(r \oplus e) = W(\tilde{r} \oplus e) \tag{26}$$

and (26) constitutes a *reductio ad absurdum*.

J. PROOF OF THEOREM 3

From [26, Th. 3] and Lemma 4, we have that any routing protocol based on Dijkstra or Bellman-Ford algorithms used in conjunction with the metric $W(r_{i,j}) = \xi_{r_{i,j}}(T^{\mathrm{CH}})$ converges to a *local-optimal route* for any network. A route $r_{i,j}$ between v_i and v_j is defined *local-optimal route* if:

$$W(r_{i,k} \oplus r_{k,j}) < W(\tilde{r}_{i,k} \oplus r_{k,j}) \quad \forall v_k \in r_{i,j},\ \forall \tilde{r}_{i,k} \neq r_{i,k} \tag{27}$$

However, a local-optimal route can be sub-optimal when the isotonicity property does not hold [26]. As an example, let us consider the topology of Figure 7, with $W(r^1_{2,j}) > W(r^2_{2,j})$ and $W(r^1_{i,j}) < W(r^2_{i,j})$. In such a case, Dijkstra or Bellman-Ford algorithms would converge toward the local-optimal route $r^1_{i,j}$ rather than the optimal route $r^*_{i,j} = r^2_{i,j}$.

Differently, the routing protocol given in Algorithm 3 is based on link-state routing, with the graph $G = (V, E)$ describing the quantum network available at each node. Furthermore, each node can converge toward the optimal path $r^*_{i,j}$ through the enumeration of all the available paths $\{r_{i,j}\} \in G$, by choosing the path with the highest end-to-end entanglement rate. With reference to previous example depicted in Figure 7, by adopting the routing protocol given in Algorithm 3, node v_i locally enumerates the two available paths $r^1_{i,j}$ and $r^2_{i,j}$, and it correctly selects the path maximizing the entanglement rate.

K. PROOF OF COROLLARY 3

First, we observe that the auxiliary function enumeratePath$(\cdot)$ can be incorporated with the main function optimalPath$(\cdot)$. By doing so, we have 4 nested *for* loops, with the outer 3 loops cycling on V and the inner loop cycling on $R(i, j)$ twice. By observing that the inner cycle is upper bounded by the number S of simple paths in G and by accounting for Corollary 1, we have the thesis.

REFERENCES

[1] A. Hellemans, "Europe bets €1 billion on quantum tech [News]," *IEEE Spectr.*, vol. 53, no. 7, pp. 12–13, Jul. 2016.

[2] C. Vu and M. Fay, "IBM builds its most powerful universal quantum computing processors," IBM, Armonk, NY, USA, Tech. Rep. pressrelease/52403, May 2017.

[3] S. Boixo *et al.* (Jul. 2016). "Characterizing quantum supremacy in near-term devices." [Online]. Available: https://arxiv.org/abs/1608.00263

[4] R. Courtland, "Google aims for quantum computing supremacy [News]," *IEEE Spectr.*, vol. 54, no. 6, pp. 9–10, Jun. 2017.

[5] H. J. Kimble, "The quantum internet," *Nature*, vol. 453, no. 7198, pp. 1023–1030, Jun. 2008.

[6] H. V. Nguyen *et al.*, "Towards the quantum Internet: Generalised quantum network coding for large-scale quantum communication networks," *IEEE Access*, vol. 5, pp. 17288–17308, 2017.

[7] Q.-C. Sun *et al.*, "Quantum teleportation with independent sources and prior entanglement distribution over a network," *Nature Photon.*, vol. 10, no. 10, pp. 671–675, Oct. 2016.

[8] J. Yin *et al.*, "Satellite-based entanglement distribution over 1200 kilometers," *Science*, vol. 356, no. 6343, pp. 1140–1144, 2017.

[9] H.-J. Briegel, W. Dür, J. I. Cirac, and P. Zoller, "Quantum repeaters: The role of imperfect local operations in quantum communication," *Phys. Rev. Lett.*, vol. 81, pp. 5932–5935, Dec. 1998.

[10] W. Dür, H.-J. Briegel, J. I. Cirac, and P. Zoller, "Quantum repeaters based on entanglement purification," *Phys. Rev. A, Gen. Phys.*, vol. 59, pp. 169–181, Jan. 1999.

[11] M. Żukowski, A. Zeilinger, M. A. Horne, and A. K. Ekert, "'Event-ready-detectors' bell experiment via entanglement swapping," *Phys. Rev. Lett.*, vol. 71, pp. 4287–4290, Dec. 1993.

[12] D. Deutsch *et al.*, "Quantum privacy amplification and the security of quantum cryptography over noisy channels," *Phys. Rev. Lett.*, vol. 77, pp. 2818–2821, Sep. 1996.

[13] W. K. Wootters and W. H. Zurek, "A single quantum cannot be cloned," *Nature*, vol. 299, no. 5886, pp. 802–803, 1982.

[14] D. Dieks, "Communication by epr devices," *Phys. Rev. A, Gen. Phys.*, vol. 92, no. 6, pp. 271–272, 1982.

[15] C. H. Bennett, G. Brassard, C. Crépeau, R. Jozsa, A. Peres, and W. K. Wootters, "Teleporting an unknown quantum state via dual classical and Einstein-Podolsky-Rosen channels," *Phys. Rev. Lett.*, vol. 70, pp. 1895–1899, Mar. 1993.

[16] T. Bacinoglu, B. Gulbahar, and O. B. Akan, "Constant fidelity entanglement flow in quantum communication networks," in *Proc. IEEE Global Telecommun. Conf. GLOBECOM*, Dec. 2010, pp. 1–5.

[17] R. Van Meter *et al.*, "Path selection for quantum repeater networks," *Netw. Sci.*, vol. 3, no. 1, pp. 82–95, Dec. 2013.

[18] S. Bratzik, S. Abruzzo, H. Kampermann, and D. Bruß, "Quantum repeaters and quantum key distribution: The impact of entanglement distillation on the secret key rate," *Phys. Rev. A, Gen. Phys.*, vol. 87, p. 062335, Jun. 2013.

[19] N. K. Bernardes, L. Praxmeyer, and P. van Loock, "Rate analysis for a hybrid quantum repeater," *Phys. Rev. A, Gen. Phys.*, vol. 83, p. 012323, Jan. 2011.

[20] M. Uphoff, M. Brekenfeld, G. Rempe, and S. Ritter, "An integrated quantum repeater at telecom wavelength with single atoms in optical fiber cavities," *Appl. Phys. B, Lasers Opt.*, vol. 122, no. 3, p. 46, Mar. 2016.

[21] H. V. Nguyen *et al.*, "Network coding aided cooperative quantum key distribution over free-space optical channels," *IEEE Access*, vol. 5, pp. 12301–12317, 2017.

[22] A. G. Radnaev *et al.*, "A quantum memory with telecom-wavelength conversion," *Nature Phys.*, vol. 6, no. 11, pp. 894–899, 2010.

[23] J. Hofmann *et al.*, "Heralded entanglement between widely separated atoms," *Sci.*, vol. 337, no. 6090, pp. 72–75, 2012.

[24] S. Ritter *et al.*, "An elementary quantum network of single atoms in optical cavities," *Nature*, vol. 484, no. 7393, pp. 195–200, 2012.

[25] J. Borregaard, P. Kómár, E. M. Kessler, M. D. Lukin, and A. S. Sørensen, "Long-distance entanglement distribution using individual atoms in optical cavities," *Phys. Rev. A, Gen. Phys.*, vol. 92, p. 012307, Jul. 2015.

[26] J. L. Sobrinho, "An algebraic theory of dynamic network routing," *IEEE/ACM Trans. Netw.*, vol. 13, no. 5, pp. 1160–1173, Oct. 2005.

[27] Y. Yang and J. Wang, "Design guidelines for routing metrics in multihop wireless networks," in *Proc. IEEE INFOCOM 27th Conf. Comput. Commun.*, Apr. 2008, pp. 1615–1623.

[28] M. Lu and J. Wu, "Opportunistic routing algebra and its applications," in *Proc. IEEE INFOCOM 28th Conf. Comput. Commun.*, Apr. 2009, pp. 2374–2382.

[29] M. Caleffi, I. F. Akyildiz, and L. Paura, "OPERA: Optimal routing metric for cognitive radio ad hoc networks," *IEEE Trans. Wireless Commun.*, vol. 11, no. 8, pp. 2884–2894, Aug. 2012.

[30] F. Rubin, "Enumerating all simple paths in a graph," *IEEE Trans. Circuits Syst.*, vol. CS-25, no. 8, pp. 641–642, Aug. 1978.

[31] C. Simon *et al.*, "Quantum memories," *Eur. Phys. J. D*, vol. 58, no. 1, pp. 1–22, May 2010.

[32] D. Alanis, P. Botsinis, S. X. Ng, and L. Hanzo, "Quantum-assisted routing optimization for self-organizing networks," *IEEE Access*, vol. 2, pp. 614–632, 2014.

[33] D. Alanis, P. Botsinis, Z. Babar, S. X. Ng, and L. Hanzo, "Non-dominated quantum iterative routing optimization for wireless multihop networks," *IEEE Access*, vol. 3, pp. 1704–1728, 2015.

[34] C. Deutsch *et al.*, "Spin self-rephasing and very long coherence times in a trapped atomic ensemble," *Phys. Rev. Lett.*, vol. 105, p. 020401, Jul. 2010.

MARCELLO CALEFFI (M'12–SM'16) received the Dr. Eng. degree *summa cum laude* (Hons.) in computer science engineering from the University of Lecce, Lecce, Italy, in 2005, and the Ph.D. degree in electronic and telecommunications engineering from the University of Naples Federico II, Naples, Italy, in 2009. He was with the Broadband Wireless Networking Laboratory, Georgia Institute of Technology, Atlanta, as a Visiting Researcher. He was also with the Nano Networking Center in Catalunya (N3Cat), Universitat Politècnica de Catalunya, Barcelona, as a Visiting Researcher. Currently, he is with the National Laboratory of Multimedia Communications, National Inter-University Consortium for Telecommunications, and with the DIETI Department, University of Naples Federico II. Since 2017, he held the Italian national habilitation as an Associate Professor in telecommunications engineering. His work appeared in several premier IEEE transactions and journals, and he received multiple awards, including the Best Strategy Award, most downloaded article awards, and most cited article awards. Currently, he serves as an Editor for the IEEE Communications Letters and *Elsevier Ad Hoc Networks*; moreover, he serves as an Associate Technical Editor for the *IEEE Communications Magazine*. He has served as the chair, the TPC chair, the session chair, and the TPC member for several premier IEEE conferences. In 2017, he was appointed as a Distinguished Lecturer from the IEEE Computer Society.